Green Chemistry

PAPER

CrossMark
← click for updates

Rapid, energy-efficient synthesis of the layered carbide, Al$_4$C$_3$†

Jennifer L. Kennedy,[a,b] Timothy D. Drysdale*[a] and Duncan H. Gregory*[b]

The phase-pure binary aluminium carbide, Al$_4$C$_3$ can be synthesised *in vacuo* from the elements in 30 minutes *via* microwave heating in a multimode cavity reactor. The success of the reaction is dependent on the use of finely divided aluminium and graphite starting materials, both of which couple effectively to the microwave field. The yellow-brown powder product was characterised by powder X-ray diffraction, scanning electron microscopy/energy dispersive X-ray spectroscopy thermogravimetric-differential thermal analysis and Raman spectroscopy. Powders were composed of hexagonal single crystallites tens of microns in diameter (rhombohedral space group $R\bar{3}m$; Z = 3; a = 3.33813(5) Å, c = 25.0021(4) Å) and were stable to 1000 °C in air, argon and nitrogen. Equivalent microwave reactions of the elements in air led to the formation of the oxycarbide phases Al$_2$OC and Al$_4$O$_4$C.

Introduction

Al$_4$C$_3$ is an important compound which can have a significant impact upon the strength and structure of a variety of materials. Up to the present time, only a small number of reports referring to the synthesis and application of the phase have been published.[1–6] Al$_4$C$_3$ has a layered rhombohedral structure ($R\bar{3}m$) composed of alternating Al$_2$C and Al$_2$C$_2$ layers.[7]

Aluminium carbide often arises as an undesired degradation product which can have a significant negative impact on SiC–Al and carbon-fibre composites.[8] In fact, the synthesis of Al$_4$C$_3$ is often an unwanted consequence of other processes such as the Hall–Héroult process.[9] Conversely, the material has been found to have beneficial effects in alloy systems such as Al–SiC–Al$_4$C$_3$, Al–Al$_3$Ti–Al$_4$C$_3$, *etc.*[7,10] The dispersion of fine Al$_4$C$_3$ particles strengthens certain Al alloys[11,12] and coating Al alloy surfaces with Al$_4$C$_3$ can enhance the wear resistance of the metal significantly.[13] Al$_4$C$_3$ is a starting point for the growth of an array of structurally related compounds and materials, such as the diamond-derived (Al$_2$O$_3$–Al$_4$C$_3$–AlN) intergrowths.[14] Al$_4$C$_3$ can also act as a template for designing microstructures such as nanoscale carbons.[15] Recently the nanostructured carbide itself has been demonstrated to be a

potentially useful functional material, with 1D Al$_4$C$_3$ nanowires acting as cold electron emitters with promising field emission performance.[5,6]

With the global push to improve the green credentials of large-scale industry, a key focus of research has become the investigation of alternative synthesis and processing methods to reduce energy consumption and pollution.[16] Previous work has shown that solid state reaction times can be cut by orders of magnitude by switching from conventional heating to microwave (MW) heating processes.[17] We have shown previously that the use of microwaves can facilitate the synthesis of carbides over second timescales.[18–21] Microwaves are particularly well-suited to the synthesis and processing of carbides, with carbon acting as both a starting material and a microwave susceptor.[17]

Further attractions of MW processing are the opportunities offered to access new and metastable materials[22] and to rationalise the interaction of solids with electromagnetic fields.[23] The development of microwave synthesis in the solution state has been more rapid given the challenges associated with homogeneity and scale up in MW solid-state synthesis and materials processing.[24] To advance solid-state microwave process design there is a requirement both to develop an underpinning understanding of how microwave reactions proceed and to design instrumentation optimised for chemical reactions. Herein we report the first successful synthesis of aluminium carbide, Al$_4$C$_3$, using microwaves. The synthesis can be completed in 30 minutes using a simple multimode cavity (MMC) reactor. A combination of powder X-ray diffraction (PXD), Raman spectroscopy, thermal analysis and scanning electron microscopy (SEM) confirms that we can produce highly crystalline, oxide-free rhombohedral Al$_4$C$_3$.

[a]School of Engineering, Rankine Building, University of Glasgow, Glasgow G12 8QQ, UK. E-mail: Timothy.Drysdale@Glasgow.ac.uk
[b]WestCHEM, School of Chemistry, Joseph Black Building, University of Glasgow, Glasgow G12 8QQ, UK. E-mail: Duncan.Gregory@Glasgow.ac.uk
†Electronic supplementary information (ESI) available. See DOI: 10.1039/c4gc01277a

Results and discussion

Aluminium carbide could be synthesised from the elements in an MMC reactor in 30 minutes. Syntheses were dependent on applied power and reaction time, and demanded the use of a sealed environment *in vacuo* (Fig. 1).

Post-reaction, sample pellets were extremely hard and when ground gave a fine, yellow-brown powder. The PXD pattern of the MW-synthesised product is shown in Fig. 2. As time progresses from time zero (starting reagents) to 30 minutes it is possible to observe the appearance of reflections attributable to the carbide phase and the reduction in intensity of the reflections from the reagents. No other phase appears in the patterns suggesting no stable, observable intermediates. The final pattern reveals that essentially single phase Al_4C_3 can be synthesised in minute timescales. There is one additional reflection in the powder pattern of the product at $2\theta \sim 27°$, which can be attributed to the (200) reflection from graphite.

Given the absence of any reflections from Al, it is proposed that the graphite reflection originates from remaining susceptor. This premise was corroborated by thermogravimetric analysis (TGA) (demonstrating a weight loss after heating in air at 1000 °C) and subsequent PXD, which showed that the excess graphite had been lost (*i.e.* the absence of the (200) reflection) and indicated no evidence of Al_4C_3 oxidation. No obvious amorphous component was detected from the background in the powder diffractograms either before or after the TGA experiment. Similar TGA experiments performed under Ar or N_2 (heating to 1000 °C) and subsequent XRD, showed no evidence of oxidation or nitridation of the carbide (or indeed any other changes). These observations are consistent with a reported decomposition temperature for Al_4C_3 at much higher temperature (2150 °C) where graphite and a carbon-saturated melt are observed as products.[25]

Scanning electron microscopy images (Fig. 3) from the MMC sample showed that the product exists as well-formed micron-scale hexagonal crystallites typically 5 μm or more across. EDX data confirmed that only aluminium and carbon are present (57.2(1) at% Al, 42.8(1) at% C) and show no trace of oxygen or nitrogen across samples (see ESI†).
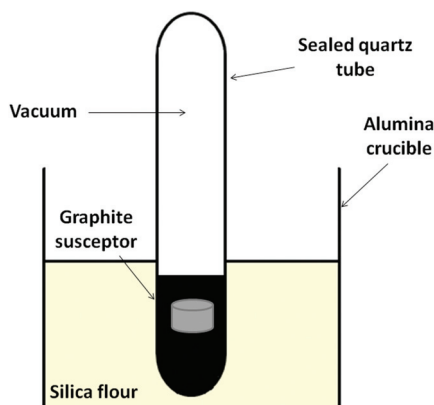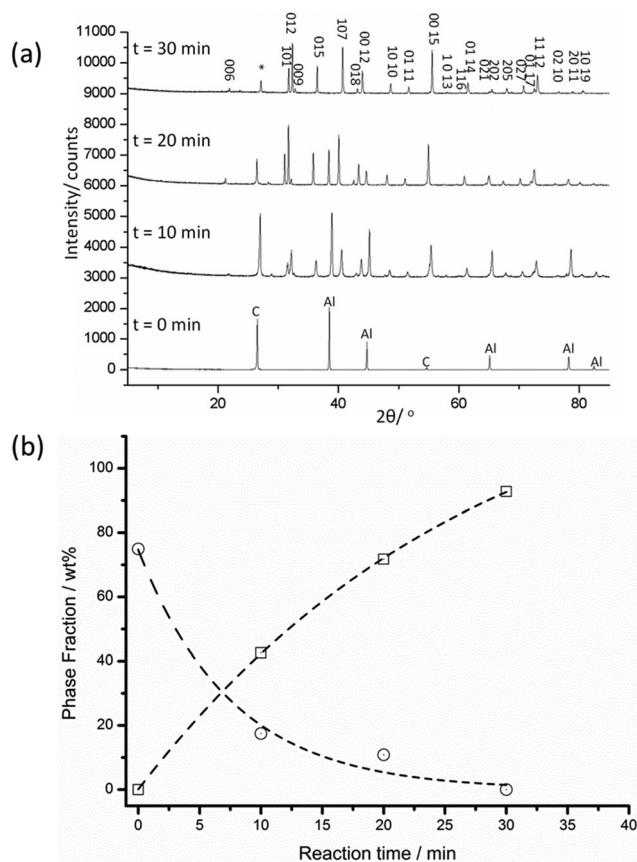

Fig. 2 (a) *Ex-situ* PXD pattern from the Al + C reaction after 0, 10, 20 and 30 min in the MMC reactor. The asterisk indicates the (002) graphite reflection; (b) refined phase fractions of Al_4C_3 (open squares) and Al (open circles) against reaction time. The behaviour can be fit approximately to sigmoidal growth and first order exponential decay functions respectively (error bars lie within the width of the plot symbols).
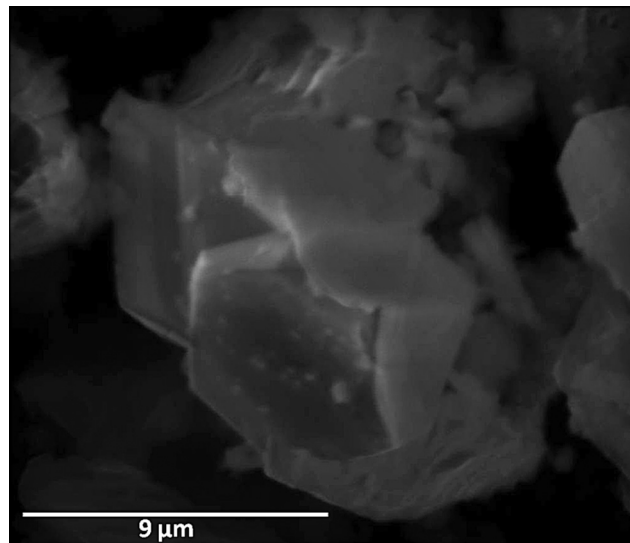

Fig. 1 Schematic of reaction set up.

Fig. 3 SEM micrograph showing well-crystallised, micron-scale hexagonal particles of Al_4C_3.

Table 1 Crystallographic data for Al_4C_3

Chemical formula	Al_4C_3
Crystal system	Rhombohedral
Space group	$R\bar{3}m$
$a/\text{Å}$	3.33813(5)
$c/\text{Å}$	25.0021(4)
Volume/Å^3	241.276(9)
Z	3
Formula weight/g mol^{-1}	143.96
Calculated density, ρ/g cm^{-3}	2.972
No. of data	6195
No. of parameters	23
R_{wp}	0.1338
R_p	0.0956
χ^2	1.861

Rietveld refinement against lab PXD data (Table 1, Fig. 4) confirmed a rhombohedral structure for Al_4C_3 based on layers of aluminium atoms interspersed with carbon atoms arranged in a regular stacking sequence.

Al_4C_3 can be considered to be a close-packed structure of aluminium atoms with a sublattice of interstitial carbon (Fig. 5). The close packed structure is a mixture of hexagonal and cubic close packed layers. Jeffrey and Wu describe the Al_4C_3 structure as consisting of $[Al_2C_2]$ and $[Al_2C]$ structural units.[2] In the case of the $[Al_2C_2]$ units the carbon atoms occupy trigonal bipyramidal interstices and the metal atoms are hexagonally stacked.[26] In the $[Al_2C]$ units, carbon atoms occupy octahedral interstices and the Al atoms form CCP layers.[26] Al atoms lie in hexagonal layers with an ...ABAB... stacking sequence switching to ...ABCB... when $z = 0$, 1/3 and 2/3.[1] Hence the metal layer stacking sequence for the unit cell is ABABCACABCBC as depicted in Fig. 5a. The refined lattice parameters are in good agreement with earlier studies of Al_4C_3 [7,27] and bond distances were close to those reported previously with Al–C distances in the range 1.927(3)–2.187(3) Å and Al–Al distances in the range 2.676(2)–2.968(1) Å (ESI†).[1,28]

Fig. 5 Crystal structure of Al_4C_3, (a) as a ball and stick representation showing Al–C bonds; (b) as a polyhedral representation showing layers Al-centred tetrahedra; (c) as a polyhedral representation showing double layers of C-centred trigonal bipyramids and single layers of C-centred compressed octahedra.

Sun et al. reported the experimental and calculated Raman spectra of Al_4C_3 in 2011[5,6] Fig. 6 shows the spectra of MW-synthesised Al_4C_3. The Raman spectrum was obtained from individual Al_4C_3 particles resolved within the sample under the Raman microscope. The spectrum is comprised of six bands, which correspond closely to those reported previously (Table 2).[5,6] There is no evidence of bands from carbon in the recorded spectra; bands for disordered (D) and ordered (graphitic; G) carbon would be expected at 1350 cm^{-1} and 1590 cm^{-1} for respectively.[29] Further, there are no bands for other Al-containing species such as the various polymorphs of Al_2O_3 [30] and hence Raman spectroscopy would support diffraction evidence that the only product of the microwave reactions is Al_4C_3.

When considering the reasons for the efficiency of the microwave reaction, it is useful to consider the way in which the reagents will interact with the applied MW field. It would be expected that both aluminium and graphite would heat principally via a conduction mechanism.[31] Graphite is well known as a very effective microwave absorber with a high
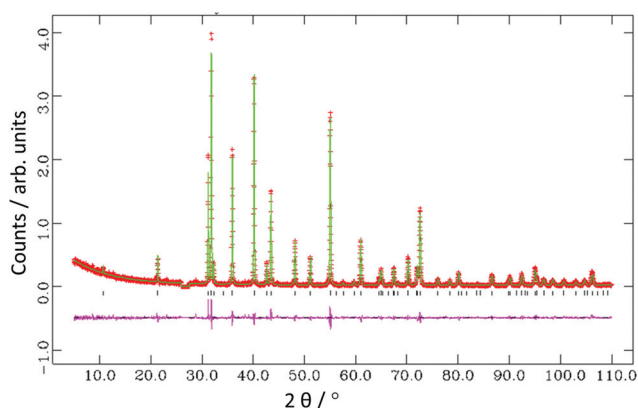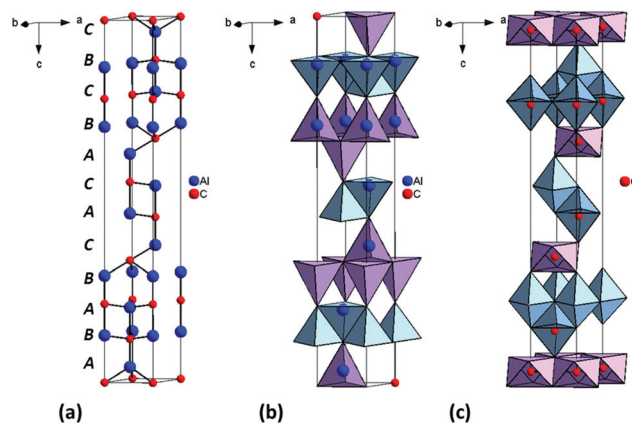

Fig. 4 Observed (plusses), calculated (solid green line), and difference (solid purple line) profile plot for the Rietveld refinement against powder XRD data for aluminium carbide. Tick marks denote Al_4C_3 diffraction peaks. The graphite reflection at $2\theta \sim 27°$ was excluded from the refinement.
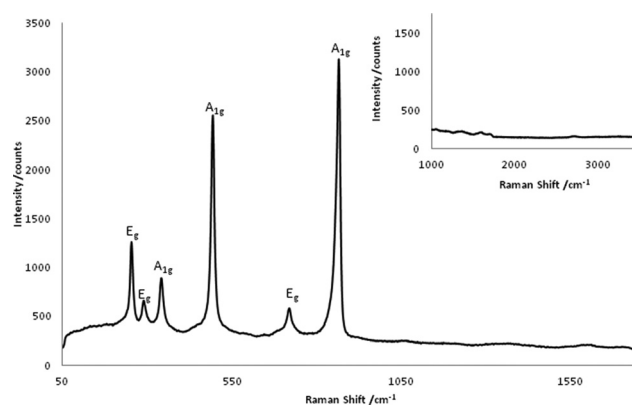

Fig. 6 Raman spectrum of Al_4C_3 showing the six characteristic bands of the carbide and the absence of carbon D and G bands (inset).

Table 2 The Raman shifts of the carbide phase and their assigned symmetry modes

Raman shift/cm^{-1}	Symmetry mode[5,6]
252.85	E_g
288.65	E_g
340.86	A_{1g}
493.00	A_{1g}
718.22	E_g
864.40	A_{1g}

dielectric loss, reaching temperatures in excess of 1000 °C in <2 min.[32] The behaviour of aluminium as a conductive metal, ($\sigma = 3.5 \times 10^7$ S m^{-1})[33] however would be expected to be highly particle size-dependent. As the microwaves penetrate further into a material, both the field intensity and power density will fall exponentially. One thus defines the penetration depth, D_p, as the distance into the material at which the power flux falls to $1/e$ of the initial value:[34]

$$D_p \approx \frac{\lambda_0 \sqrt{\varepsilon'}}{2\pi\varepsilon''} \tag{1}$$

where λ_0 is the wavelength of the microwave radiation, ε' is the dielectric constant and ε'' is the dielectric loss. The penetration depth of Al has been determined by Rodiger *et al.* to be 1.7 µm (for 2.45 GHz microwaves at 20 °C).[35] Thus, for large particle sizes one would expect a high reflectance at the surface leading to the escalation of high surface voltages. In our previous work in M–C systems (where M = W, Mo, Nb and Ta) a general behaviour in the interaction of these systems with microwaves has been observed.[19–21,36,37] This behaviour is rationalised by considering the loss tangent, $\tan\delta$ ($= \varepsilon''/\varepsilon'$), which describes the ability of a material (at a specific temperature and frequency) to absorb microwave energy and dissipate heat.[34] Initially energy is absorbed by the carbon susceptor (loss tangent up to 2.95; *cf.* loss tangent of water 0.118, at 2.45 GHz and 298 K[38]) then as the temperature increases the dielectric properties of the reactant mixture reach an optimum point where $\tan\delta$ is at a maximum. From this point product formation is rapid and the reaction self-terminating.

Given that Al$_4$C$_3$ is considered to be the only phase in the Al–C equilibrium phase system[25] and, indeed, that no other phases are observed by *ex-situ* PXD, it is postulated that the reaction mechanism is a simple one involving direct combination of the elements. However it is only *via* probing the carbide formation process *in situ* that any intermediate steps in the reaction are likely to be identified. Such insight requires the development of *in situ* analysis instrumentation to perform time-resolved experiments.[17]

Conventionally Al$_4$C$_3$ is prepared *via* direct carbonisation or carbothermal reduction–carbonisation techniques.[39–41] The carbide can be prepared by reacting stoichiometric quantities of aluminium and graphite between 1250–1500 °C under a flow of argon or by combining alumina and graphite under similar conditions at 1900 °C.[40] Optical pyrometry offers a convenient, contactless method of measuring temperature without

perturbing a microwave field. However, given the sealed tube reaction configuration shown in Fig. 1, it proved impossible to obtain valid temperature values using this method. Considering the temperatures typically required in the conventional preparation of Al$_4$C$_3$ from the elements combined with the observation of the softening of the quartz reaction vessel in our experiments, it can be assumed that that temperature in the microwave reactions here must far exceed 1000 °C.

Without doubt the practical preparative procedure would be simplified (and ultimately be made more cost-effective in scaled-up processes) if the carbide synthesis could be performed in air (as we have achieved in the MW preparation of SiC from the elements, for example[18]). Despite the presence of carbon in large excess, microwave reactions in open tube conditions resulted in the formation of phase mixtures of Al$_2$O$_3$, Al$_2$OC, Al$_4$O$_4$C and Al$_4$C$_3$ (see ESI†). This is perhaps unsurprising as the requirement of an inert environment is also essential for synthesis of Al$_4$C$_3$ *via* conventional heating processes.[40,41] The reasons for the preferential formation of oxides and oxycarbides under such conditions can perhaps be explained by the reaction processes that may occur in the presence of oxygen (Table 3).[40–42]

The extremely high enthalpy and Gibbs free energy values for the oxide and oxycarbide phases strongly support the observed requirement for an oxygen-free environment. Moreover, the oxycarbide phase Al$_2$OC has been observed to appear in carbon-rich environments[44] which may also be explained by the solid phase reaction given below (eqn (2)).[45] *In situ* evolved gas analysis would be required to verify the nature of the gaseous by-products.

$$Al_2O_3 + 3C \rightleftharpoons Al_2OC + 2CO_{(g)} \tag{2}$$
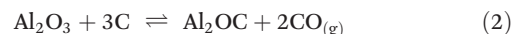
The relative stability of alumina and the aluminium oxycarbide phases above not only accounts for the difficulty in producing Al$_4$C$_3$ from the elements in air, but also contributes to the challenges involved in synthesising Al$_4$C$_3$ *via* the carbothermal reduction–carburisation of alumina (eqn (3)). Typically such processes require reaction temperatures in excess of 1800 °C.[46]

$$2Al_2O_3 + 9C \rightarrow Al_4C_3 + 6CO_{(g)} \tag{3}$$
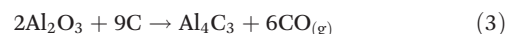
Ideally, a process exploiting earth-abundant alumina as a starting material while expending less energy in a microwave-driven synthesis route would be attractive. In this context however, the thermodynamic challenges associated with eqn (3) ($\Delta H \geq 2000$ kJ mol^{-1} (ref. 47)) are compounded by the poor dielectric properties of alumina. With a dielectric con-

Table 3 Calculated molar enthalpy (ΔH) and Gibbs free energy (ΔG) of formation of Al$_2$OC, Al$_2$O$_3$ and Al$_4$O$_4$C at 298.15 K. For comparison the enthalpy and Gibbs free energy of formation of Al$_4$C$_3$ are also shown[43]

Phase	Reaction	ΔH/kJ mol^{-1}	ΔG/kJ mol^{-1}
Al$_2$OC	$2Al + CO \rightleftharpoons Al_2OC$	−634.96	−641.09
Al$_2$O$_3$	$4Al + 3O_2 \rightleftharpoons 2Al_2O_3$	−1675.69	−1690.88
Al$_4$O$_4$C	$2Al_2O_3 + 3C \rightleftharpoons Al_4O_4C + 2CO$	−2314.32	−2343.25
Al$_4$C$_3$	$4Al + 3C \rightleftharpoons Al_4C_3$	−206.90	−232.95

stant, ε' and dielectric loss, ε'' of 9.1 and 0.004 respectively,[48] although the penetration depth of alumina is far superior to aluminium (10 m $vs.$ 1.7 μm),[35] the loss tangent is orders of magnitude lower. Hence, it is only at elevated temperature that Al_2O_3 begins to heat effectively in a microwave field. These factors present a convincing argument for single mode cavity (SMC) microwave synthesis in which the power density within the sample can be controlled more efficiently. Previous experiments have demonstrated that reactions forming carbides are self-terminating and circumvent, for example, problems with thermal runway in oxide starting materials such as alumina.[17] The design of such SMC processes will be a subject of our future investigations.

Experimental

Synthesis

Stoichiometric amounts of powders of aluminium (Sigma Aldrich, (99.9%)) and graphite (Sigma Aldrich, <20 mm, synthetic) (4 : 3 molar ratio, typical mass 0.5 g) were ground in a mortar and pestle for 10 minutes. The dry, ground powders were pressed in an 8 mm pellet die (Medway Optics, 5 tonnes, 10 min) without use of a binder. Pellets were embedded in graphite (acting as a MW susceptor) in a 10 mm diameter quartz tube which was then evacuated and sealed. Synthesis experiments were conducted in a multimode microwave cavity reactor (Sharp R272WM, 800 W, 2.45 GHz) in which the microwave field was mapped iteratively using graphite.

Characterisation

Products were characterised by PXD (PANalytical Xpert MPD, Cu Kα1 radiation; collected for 1–12 h over a range of $5 < 2\theta/° < 85$ with a step size of 0.0167° 2θ)) and data used to identify product phases (by comparison with the ICDD PDF database using the PANalytical program X'pert HighScore Plus).

Structures were refined by the Rietveld method against PXD data (collected for 12 h over a range of $5 \leq 2\theta/° \leq 110$ with a step size of $2\theta = 0.0167°$) using the GSAS and EXPGUI software.[49,50] Rietveld refinements were performed using the previously described rhombohedral $R\bar{3}m$ structure of Al_4C_3 as a starting model.[27] The background (modelled using a shifted Chebyschev function; function 1 within GSAS), scale factor, zero point and cell parameters were refined in initial cycles. Peak widths and profile coefficients (peak shape was modelled using the pseudo Voigt function; peak shape function 2 within GSAS) and isotropic temperature factors were subsequently refined. The observed (200) reflection from graphite (27° 2θ) was excluded from the profile as the inclusion of this impurity phase peak caused the refinement to diverge. Otherwise all refinements converged smoothly in final cycles. We find no evidence of oxygen-inclusion in the bulk material or in the form of additional oxide phases. This is corroborated by Energy-dispersive X-ray Spectroscopy (EDX; see below) data, which confirm that only aluminium and carbon are present.

Thermogravimetric analysis (TGA) measurements were performed using a TA Instruments Q500 gravimetric analyser. Samples were heated in platinum pans from ambient temperature to 1000 °C at a rate of 10 °C min^{-1}, with the mass of the sample recorded as a function of temperature. Measurements were carried in air, flowing Ar and flowing N_2 respectively.

Raman data were collected at room temperature using a Horiba LabRAM confocal microscope system with a 532 nm green laser. A hole aperture of 50 μm, 600 g mm^{-1} grating and a synapse CCD detector were employed. Sample morphology and composition were studied using SEM (Hitachi S4700 microscope, 20 kV accelerating voltage). An Oxford Instruments X-act spectrometer was coupled to this microscope for EDX analysis. The instrument is calibrated using the INCA EDX analysis software (Cu used for all calibration measurements) and the software also allows selection of regions for analysis and definition of measurement parameters.

Conclusions

In summary, high-purity aluminium carbide has been synthesised over rapid timescales ($cf.$ 12 h at 1500 °C required conventionally[39]) The applied microwave power and the atmosphere in which the reaction is conducted are key variables in the synthesis of the carbide in the absence of oxides or oxycarbides. Reduction of the applied power means that the reaction either (1) will not proceed or (2) will be inefficient with incomplete conversion of starting materials. PXD and Raman spectroscopy confirm the formation of the carbide phase and indicate that high-purity products can be obtained. The structure of Al_4C_3 has been confirmed by Rietveld refinement against PXD data and shows no significant differences to that of the conventionally-prepared carbide. SEM has shown that the phase exists as micron-scale hexagonal crystallites and EDX analysis confirmed that only aluminium and carbon were present. It is expected that this easily-implemented experimental methodology may be applied to the formation of other more complex carbide materials based on the layered structure of Al_4C_3. Ultimately, it will be exciting to observe how the composition, crystal chemistry and microstructure might be controlled via microwave synthesis parameters and to what extent both structural and functional properties can be influenced.

Acknowledgements

Notes and references

1 G. A. Jeffrey and V. Y. Wu, $Acta\ Crystallogr.$, 1966, **20**, 538.
2 G. A. Jeffrey and V. Y. Wu, $Acta\ Crystallogr.$, 1963, **16**, 559.

3 H. F. Zhang, A. C. Dohnalkova, C. M. Wang, J. S. Young, E. C. Buck and L. S. Wang, *Nano Lett.*, 2002, **2**, 105.

4 C. N. He, N. Q. Zhao, C. S. Shi and S. Z. Song, *Carbon*, 2010, **48**, 931.

5 Y. Sun, H. Cui, L. Gong, J. Chen, P. K. Shen and C. X. Wang, *Nanoscale*, 2011, **3**, 2978.

6 Y. Sun, H. Cui, L. Gong, J. A. Chen, J. C. She, Y. M. Ma, P. K. Shen and C. X. Wang, *ACS Nano*, 2011, **5**, 932.

7 V. L. Solozhenko and O. O. Kurakevych, *Solid State Commun.*, 2005, **133**, 385.

8 C. Ji, Y. Z. Ma, M. C. Chyu, R. Knudson and H. Y. Zhu, *J. Appl. Phys.*, 2009, **106**, 083511.

9 J. Q. Li, G. Q. Zhang, D. S. Liu and O. Ostrovski, *ISIJ Int.*, 2011, **51**, 870.

10 P. S. Gilman and J. S. Benjamin, *Annu. Rev. Mater. Sci.*, 1983, **13**, 279.

11 T. Hasegawa, T. Miura, T. Takahashi and T. Yakou, *ISIJ Int.*, 1992, **32**, 902.

12 M. Besterci, L. Pesek, P. Zubko and P. Hvizdos, *Mater. Lett.*, 2005, **59**, 1971.

13 F. Fariaut, C. Boulmer-Leborgne, E. Le Mann, T. Sauvage, C. Andreazza-Vignolle, P. Andreazza and C. Langlade, *Appl. Surf. Sci.*, 2002, **186**, 105.

14 W. A. Groen, M. J. Kraan, P. F. vanHal and A. E. M. DeVeirman, *J. Solid State Chem.*, 1995, **120**, 211.

15 J. Leis, A. Perkson, M. Arulepp, M. Kaarik and G. Svensson, *Carbon*, 2001, **39**, 2043.

16 M. Poliakoff, J. M. Fitzpatrick, T. R. Farren and P. T. Anastas, *Science*, 2002, **297**, 807.

17 H. J. Kitchen, S. R. Vallance, J. L. Kennedy, N. Tapia-Ruiz, L. Carassiti, A. Harrison, A. G. Whittaker, T. D. Drysdale, S. W. Kingman and D. H. Gregory, *Chem. Rev.*, 2014, **114**, 1170.

18 L. Carassiti, A. Jones, P. Harrison, P. S. Dobson, S. Kingman, I. MacLaren and D. H. Gregory, *Energy Environ. Sci.*, 2011, **4**, 1503.

19 S. R. Vallance, S. Kingman and D. H. Gregory, *Adv. Mater.*, 2007, **19**, 138.

20 S. R. Vallance, S. Kingman and D. H. Gregory, *Chem. Commun.*, 2007, 742.

21 S. R. Vallance, H. J. Kitchen, C. Ritter, S. Kingman, G. Dimitrakis and D. H. Gregory, *Green Chem.*, 2012, **14**, 2184.

22 A. G. Whittaker, A. Harrison, G. S. Oakley, I. D. Youngson, R. K. Heenan and S. M. King, *Rev. Sci. Instrum.*, 2001, **72**, 173.

23 A. G. Whittaker, *Chem. Mater.*, 2005, **17**, 3426.

24 M. D. Bowman, J. L. Holcomb, C. M. Kormos, N. E. Leadbeater and V. A. Williams, *Org. Process Res. Dev.*, 2008, **12**, 41.

25 C. Qiu and R. Metselaar, *J. Alloys Compd.*, 1994, **216**, 55.

26 A. Feldhoff, E. Pippel and J. Woltersdorf, *Philos. Mag. A*, 1999, **79**, 1263.

27 T. M. Gesing and W. Jeitschko, *Z. Naturforsch., B: Chem. Sci.*, 1995, **50**, 196.

28 T. M. Gesing and W. Jeitschko, *J. Solid State Chem.*, 1998, **140**, 396.

29 M. J. Matthews, M. A. Pimenta, G. Dresselhaus, M. S. Dresselhaus and M. Endo, *Phys. Rev. B: Condens. Matter*, 1999, **59**, R6585.

30 P. V. Thomas, V. Ramakrishnan and V. K. Vaidyan, *Thin Solid Films*, 1989, **170**, 35.

31 C. O. Kappe, *Angew. Chem., Int. Ed.*, 2004, **43**, 6250.

32 K. J. Rao, B. Vaidhyanathan, M. Ganguli and P. A. Ramakrishnan, *Chem. Mater.*, 1999, **11**, 882.

33 R. A. Serway, *Principles of Physics*, Saunders College Publishing, Fort Worth, Texas, 2 edn, 1998.

34 A. C. Metaxas and R. J. Meredith, *Industrial Microwave Heating*, Peter Peregrinus Ltd, London, 1983.

35 K. Rodiger, K. Dreyer, T. Gerdes and M. Willert-Porada, *Int. J. Refract. Met. Hard Mater.*, 1998, **16**, 409.

36 S. R. Vallance, *Microwave synthesis and mechanistic examination of transition metal carbides*, PhD thesis, University of Nottingham, 2008.

37 S. R. Vallance, D. M. Round, C. Ritter, E. J. Cussen, S. Kingman and D. H. Gregory, *Adv. Mater.*, 2009, **21**, 4502.

38 J. A. Menendez, A. Arenillas, B. Fidalgo, Y. Fernandez, L. Zubizarreta, E. G. Calvo and J. M. Bermudez, *Fuel Process. Technol.*, 2010, **91**, 1.

39 K. Itatani, M. Hasegawa, M. Aizawa, E. S. Howell, A. Kishioka and M. Kinoshita, *J. Am. Ceram. Soc.*, 1995, **78**, 801.

40 J. H. Cox and L. M. Pidgeon, *Can. J. Chem.*, 1963, **41**, 671.

41 P. Lefort, D. Tetard and P. Tristant, *J. Eur. Ceram. Soc.*, 1993, **12**, 123.

42 J. M. Lihrmann, *J. Eur. Ceram. Soc.*, 2008, **28**, 633.

43 C. Qiu and R. Metselaar, *Z. Metallkd.*, 1995, **86**, 198.

44 L. M. Foster, G. Long and M. S. Hunter, *J. Am. Ceram. Soc.*, 1955, **39**, 1.

45 H.-b. Yuan, B. Yang, B.-q. Xu, Q.-c. Yu, Y.-b. Feng and Y.-n. Dai, *Trans. Nonferrous Met. Soc. China*, 2010, **20**, 1505.

46 *Aluminum Recycling and Processing for Energy Conservation and Sustainability*, ed. J. A. S. Green, ASM International Ohio, 2007.

47 M. Heyrman and C. Chatillon, *J. Electrochem. Soc.*, 2006, **153**, E119.

48 A. J. Berteaud and J. C. Badot, *J. Microw. Power Electromagn. Energy*, 1976, **11**, 315.

49 A. C. Larson and R. B. Von Dreele, General Structure Analysis System (GSAS), *Los Alamos National Laboratory Report LAUR 86-748*, 2004.

50 B. H. Toby, *J. Appl. Crystallogr.*, 2001, **34**, 210.